

Two-Dimensional Scan of the Performance of Generalized Gradient Approximations with Perdew–Burke–Ernzerhof-Like Enhancement Factor

E. Fabiano,^{*†} Lucian A. Constantin,[‡] and F. Della Sala^{†,‡}

[†]National Nanotechnology Laboratory (NNL), Istituto Nanoscienze—CNR, Via per Arnesano 16, I-73100 Lecce, Italy

[‡]Center for Biomolecular Nanotechnologies @UNILE, Istituto Italiano di Tecnologia (IIT), Via Barsanti, I-73010 Arnesano, Italy

 Supporting Information

ABSTRACT: We assess the performance of the whole class of functionals defined by the Perdew–Burke–Ernzerhof (PBE) exchange-correlation enhancement factor, by performing a two-dimensional scan of the μ and κ parameters (keeping β fixed by the recovery of the local density approximation linear response). We consider molecular (atomization energies, bond lengths, and vibrational frequencies), intermolecular (hydrogen-bond and dipole interactions), and solid-state (lattice constant and cohesive energies) properties. We find, for the energetical properties, a whole family of functionals (with μ and κ interrelated) giving very similar results and the best accuracy. Overall, we find that the original PBE and the recently proposed APBE functional [*Phys. Rev. Lett.* **2011**, *106*, 186406], based on the asymptotic expansion of the semiclassical neutral atom, give the highest global accuracy, with a definite superior performance of the latter for all of the molecular properties.

1. INTRODUCTION

Ground-state density functional theory^{1,2} (DFT) in the Kohn–Sham³ (KS) self-consistent formalism is nowadays one of the most popular computational methods in electronic calculations of quantum chemistry and solid-state physics. The central quantity in DFT is the exchange-correlation (XC) functional, which collects all of the “unknown” terms of the electron–electron interaction. Over the years, many approximations have been developed for the XC functional, which form the so-called “Jacob’s ladder” of DFT.⁴

The ladder is grounded on the Hartree approximation (i.e., no XC contribution) and has at the first rung the local spin-density approximation³ (LSDA), which only contains as ingredients the electron spin-densities $\rho_{\uparrow}(\mathbf{r})$ and $\rho_{\downarrow}(\mathbf{r})$. The second rung of the ladder is formed by those functionals depending on the gradient of the electron spin-densities ($\nabla \rho_{\uparrow}(\mathbf{r})$, $\nabla \rho_{\downarrow}(\mathbf{r})$) as well as on the electron spin-densities themselves. The generalized gradient approximations⁵ (GGAs) and the second-order gradient expansions, derived from small perturbations of the uniform electron gas (GE2)⁶ or from the semiclassical theory of neutral atoms (MGE2),^{7–12} are the most important representatives of this class. On the third rung of Jacob’s ladder, formed by meta-GGAs, the additional ingredients of the positive KS kinetic energy spin-densities ($\tau_{\uparrow}(\mathbf{r})$, $\tau_{\downarrow}(\mathbf{r})$) or the Laplacian of the spin-densities ($\nabla^2 \rho_{\uparrow}(\mathbf{r})$, $\nabla^2 \rho_{\downarrow}(\mathbf{r})$) are considered, in order to satisfy more exact constraints of the XC energy and potential. On the fourth rung, the dependence on occupied KS orbitals is taken into account, in search of an improved description of the exchange energy or of a fully nonlocal correlation energy compatible with exact exchange.¹³ Hybrid¹⁴ and orbital-dependent^{15–17} functionals, as well as hyper-GGAs,¹³ belong to this rung. Finally, on the fifth rung of the ladder, we find functionals including an explicit

dependence on virtual KS orbitals,^{18–23} which allow one to describe exactly nonlocal parts of the correlation energy density.

Despite the remarkable accuracy demonstrated by the functionals belonging to the fourth and fifth rungs of Jacob’s ladder in different test studies, the majority of practical DFT applications are based on GGAs and hybrid functionals, which provide the best compromise between accuracy and computational effort. In particular, GGA functionals provide an efficient tool for the study of large systems (e.g., for biology and solid-state physics) and still outperform hybrid functionals for organometallic and transition metal complexes.^{24–27} In addition, they attract basic theoretical interest, because they constitute the basis on which meta-GGA, hyper-GGA, and hybrid functionals are constructed.

Among different GGA functionals, the generalized gradient approximation proposed in 1986 by Perdew, Burke, and Ernzerhof (PBE)²⁸ has gained large popularity in both quantum chemistry and condensed-matter physics, due to its simplicity and good performance in a broad range of applications. The PBE functional contains no empirical parameters and fulfills a number of exact constraints for the XC energy. The correlation part of the PBE functional was constructed from a sharp cutoff of the GE2 correlation hole (in the high density limit)²⁹ and is defined as

$$E_c^{\text{PBE}}[\rho_{\uparrow}, \rho_{\downarrow}] = \int \rho [\varepsilon_c^{\text{unif}}(r_s, \xi) + H(r_s, \xi, t)] d\mathbf{r} \quad (1)$$

where

$$H(r_s, \xi, t) = \gamma \phi^3 \ln \left(1 + \frac{\beta}{\gamma} \frac{t^2 + At^4}{1 + At^2 + A^2 t^4} \right) \quad (2)$$

Received: July 26, 2011

Published: September 20, 2011

with $\rho = \rho_\uparrow + \rho_\downarrow$ being the total electron density, $r_s = [(4\pi/3)\rho]^{1/3}$ being the local Seitz radius, $\zeta = (\rho_\uparrow - \rho_\downarrow)/\rho$ being the relative spin polarization, $\phi = ((1 + \zeta)^{2/3} + (1 - \zeta)^{2/3})/2$ being a spin scaling factor, $\varepsilon_c^{\text{unif}}(r_s, \zeta)$ being the correlation energy per particle of the uniform electron gas, A being a function of $\varepsilon_c^{\text{unif}}$ and ϕ , and $t = |\nabla \rho|/(2\phi k_F \rho)$ being the correlation density gradient that measures the density variations over a Thomas–Fermi screened wave-number $k_s = (4k_F/\pi)^{1/2}$, where $k_F = (3\pi^2\rho)^{1/3}$ is the Fermi wave vector. The parameter $\gamma = (1 - \ln 2)/\pi^2 \approx 0.031091$ is fixed by uniform scaling to the high-density limit of the (spin-unpolarized) correlation energy, and the parameter $\beta = \beta^{\text{PBE}} = 0.066725$ is the second-order gradient expansion coefficient of the correlation energy in the high-density limit.

The exchange part of the PBE functional has as the enhancement factor a simple Padé-polynomial formula originally proposed by Becke:³⁰

$$F_x^{\text{PBE}}(s) = 1 + \kappa - \frac{\kappa}{1 + \frac{\mu s^2}{\kappa}} \quad (3)$$

where $s = |\nabla \rho|/(2k_F \rho)$ is the reduced gradient. The exchange energy for a spin-unpolarized system is then

$$E_x^{\text{PBE}}[\rho] = \int \rho \varepsilon_x^{\text{unif}}(\rho) F_x^{\text{PBE}}(s) \, d\mathbf{r} \quad (4)$$

where $\varepsilon_x^{\text{unif}}(\rho)$ is the exchange energy per particle of the uniform electron gas, while for any spin-polarized system

$$E_x[\rho_\uparrow, \rho_\downarrow] = \frac{E_x[2\rho_\uparrow] + E_x[2\rho_\downarrow]}{2} \quad (5)$$

from the spin-scaling relation of the exchange energy.³¹

The exchange enhancement factor in eq 3 is very simple and satisfies two important limits: for small s , we have $F_x^{\text{PBE}}(s) \approx 1 + \mu s^2$; while for large s , $F_x^{\text{PBE}}(s) \rightarrow 1 + \kappa$. The parameter $\kappa = \kappa^{\text{PBE}} = 0.804$ is fixed by the Lieb–Oxford bound for the exchange energy, and the parameter μ is fixed to satisfy the correct linear response of the spin-unpolarized uniform electron gas, i.e.

$$\mu = \beta \frac{\pi^2}{3} \quad (6)$$

which leads to $\mu = \mu^{\text{PBE}} = 0.21951$.

Since its introduction, many variations of the original PBE functional have been presented.^{12,32–45} Some of them keep the same functional form for the exchange and correlation but employ different parameters.^{12,32,35,37,38,41,43} These functionals can be represented by a triplet of parameters $(\mu; \beta; \kappa)$, see also ref 46. Among them, we recall:

- (i) revPBE,³² an empirical functional constructed for molecules with

$$(\mu = \mu^{\text{PBE}}; \beta = \beta^{\text{PBE}}; \kappa = 1.245)$$

where κ was fitted to atoms

- (ii) PBEsol,^{37,38} a functional for solids and surfaces, with

$$\left(\mu = \mu^{\text{GE2}} = \frac{10}{81}; \beta = 0.046; \kappa = \kappa^{\text{PBE}} \right)$$

where μ^{GE2} is the exact second-order gradient expansion coefficient of the exchange energy and β was fitted to jellium surfaces

- (iii) APBE,¹² a nonempirical functional accurate for molecular systems, constructed from the semiclassical theory

of neutral atoms, with

$$\left(\mu = \mu^{\text{MGE2}} = 0.26; \beta = \frac{3\mu^{\text{MGE2}}}{\pi^2} = 0.079; \kappa = \kappa^{\text{PBE}} \right)$$

where μ^{MGE2} is the coefficient of the modified second-order gradient expansion and β was chosen to recover the LSDA linear response. We note that the construction of the APBE functional shares some similarities with that of PBE(Jr,Gx).⁴¹ However, the latter uses $\mu = \mu^{\text{GE2}} = 10/81$, recovering GE2 and not MGE2. It thus behaves similarly to PBEsol and rather differently than APBE. This fact highlights the importance of the modified second-order gradient expansion for the exchange in the construction of APBE.

Other functionals modify the functional form of the exchange enhancement factor,^{33,34,36,39,40,42,44,44,45} often producing a faster increase of $F_x^{\text{PBE}}(s)$ with s . Of particular relevance we recall the following: Wu–Cohen (WC)³⁶ and the second-order GGA⁴⁰ (developed for better solid-state properties), PBEint⁴⁴ and RPBE³³ (developed for hybrid interfaces), and the regularized gradient expansion.⁴² These functionals can also be written as a parameter triplet provided that μ is expressed as a function of s . For the PBEint functional, e.g., we have

$$\left(\mu = \mu(s) = \mu^{\text{GE2}} + \frac{(\mu^{\text{PBE}} - \mu^{\text{GE2}})as^2}{1 + as^2}; \beta = 0.052; \kappa = \kappa^{\text{PBE}} \right)$$

where $a = (\mu^{\text{GE2}})^2 / (\kappa(\mu^{\text{PBE}} - \mu^{\text{GE2}})) = 0.197$ is determined by the requirement of a smooth functional derivative. Thus, $\mu(s)$ interpolates between the GE2 and PBE coefficients, whereas β is fitted to jellium surfaces.

By changing the parameters in the PBE functional form, important exact constraints for solids, surfaces, or molecular systems can be recovered, and improved accuracy can be achieved for special classes of problems. However, it is not possible to satisfy all of the different constraints at once. In fact, no GGA functional can be accurate for both solid-state properties and atoms.¹⁰

In recent years, many different investigations about the performance of the PBE-like functionals have been presented.^{46,47} Some studies focused on the relevance of the κ parameter,^{40,48} the μ parameter,⁴⁶ or both.^{12,37,38,41} However, so far, only few points in the three-dimensional $(\mu; \beta; \kappa)$ space have been investigated and mainly for few selected properties.⁴⁶

In this paper, we aim at critically assessing this issue and explore the dependence of the performance of a whole family of PBE-like functionals on the values of the μ and κ parameters. For the sake of clarity, we restricted our attention to those PBE-like functionals that satisfy the LSDA linear response. This choice is also motivated by the fact that this is the only known exact constraint for the correlation energy of importance for molecular or solid-state systems. The second-order gradient expansion for the correlation has been in fact demonstrated to be of minor importance for real systems.⁴⁹ Therefore, we performed a two-dimensional scan of PBE-functionals of the type

$$[\mu, \kappa] = \left(\mu; \beta = \frac{3\mu}{\pi^2}; \kappa \right)$$

Previous studies⁴¹ and preliminary test calculations (see the Supporting Information) indicate that different choices of β do not modify the results significantly. Nevertheless, we

cannot exclude more important effects for particular properties and/or systems.

We consider many different tests, namely, atomization energies and bond lengths of organic molecules, transition metals, and metal complexes; harmonic vibrational frequencies of organic molecules; binding energies of hydrogen-bonded and dipole-interacting molecular systems; equilibrium lattice constants; and cohesive energies of solids. For each test, the results are presented as contour graphs showing the accuracy of the PBE-like functionals for different combinations of the (μ, κ) parameters, and the performance of standard PBE-like functionals (i.e., PBE, APBE, revPBE) is analyzed. In addition, global errors for different classes of problems are considered. We find that the nonempirical APBE and PBE functionals are the most representative functionals for a broad palette of properties and systems and yield the higher accuracy over a large number of tests. In addition, APBE outperforms PBE for molecular properties.

We note finally that, of course, for practical reasons, our selection of tests is necessarily limited. For example, it does not consider quantities such as transition barriers, isomerization energies, or reaction energies, just to mention a few relevant to the ground-state energetics. At the same time, for computational reasons, it is essentially restricted to considering small molecules, while tests including large organic molecules^{43,50} or extended metal systems are not considered (these would require in addition the consideration of further theoretical issues as for example dispersion corrections⁵¹). This facts suggest that caution must be used in drawing conclusions from the present work, as from any other similar broad-range assessment work, because of a possible bias introduced by the selection of specific test sets (see in this respect the discussion in ref 52). Nevertheless, we believe that the present selection of tests is representative of a fairly large class of the most fundamental and important problems in quantum chemistry and solid-state physics and can thus provide useful insight into the performance of the family of PBE-like functionals.

2. COMPUTATIONAL DETAILS

Several properties of molecules and bulk solids were investigated by employing a PBE-like functional (eqs 1–6) with μ and κ values in the intervals $\mu \in [0.1, 0.3]$ and $\kappa \in [0.5, 1.5]$ and the β parameter fixed by the relation $\beta = 3\mu/\pi^2$ in order to preserve the accurate LSDA linear response. The parameter μ (κ) was varied in steps of 0.01 (0.1). In total, we tested 231 different PBE-like functionals.

We considered the following properties and test sets:
AE6: Atomization energies were computed for SiH₄, SiO, S₂, CH₄, C₂O₂H₂, and C₄H₈; accurate reference data were taken from ref 53.

TMAE4: Atomization energies were computed for the Cr₂, Cu₂, V₂, and Ag₂ transition metal complexes; reference data were taken from ref 25.

MCAE6: Atomization energies were calculated for the AgH, BeO, FeS, LiCl, MgO, and VS metal complexes; reference data were obtained from ref 26.

HBL9: Optimization of bond lengths involving at least one hydrogen atom are provided. The following molecules were considered: H₂, CH₄, NH₃, H₂O, HF, C₂H₂ (C–H bond), HCN (C–H bond), H₂CO (C–H bond), and OH; reference values were taken from ref 54.

NHBL10: Bond lengths were optimized for CO, N₂, F₂, C₂H₂ (C–C bond), HCN (C–N bond), H₂CO (C–O bond), CO₂, N₂O, and Cl₂; reference values were taken from ref 54.

TMBL4: Bond lengths were computed for the Cr₂, Cu₂, V₂, and Ag₂ transition metal complexes; reference data were taken from ref 25.

MCBL6: Bond lengths were optimized for the AgH, BeO, FeS, LiCl, MgO, and VS metal complexes; reference data were obtained from ref 26.

F38: Harmonic vibrational frequencies were calculated for H₂, CH₄, NH₃, H₂O, HF, CO, N₂, F₂, C₂H₂, HCN, H₂CO, CO₂, N₂O, Cl₂, and OH; reference data were obtained from ref 55.

HB6/04: The binding energies of hydrogen-bond interacting systems were calculated for (H₂O)₂, (HCONH₂)₂, (HCOOH)₂, (HF)₂, (NH₃)₂, and NH₃–H₂O; reference data were taken from ref 56.

D16/04: The binding energies of dipole-interacting systems were calculated for CH₃Cl–HCl, CH₃SH–HCl, CH₃SH–NCH, (H₂S)₂, (HCl)₂, and H₂S–HCl; reference data were taken from ref 56.

SOLIDS: Equilibrium lattice constants and cohesive energies were computed for bulk Na (simple metal), Ag, Cu (transition metals), Si, GaAs (semiconductors), and NaCl (ionic solid); reference values were taken from refs 47 and 57. This small test of six solids can reproduce the mean absolute errors of the functionals for larger set of solids well.⁴⁴ For example, for 60 solids,⁴⁵ the PBE lattice constant mean absolute error is 0.054 Å, whereas our small test of solids gives a PBE error of 0.0597 Å.

In all calculations, fully relaxed geometries were considered. The simulations of molecular systems were performed with the TURBOMOLE program package,⁵⁸ using a def2-TZVPP^{59,60} basis set. The simulations of solid-state properties were performed employing the FHI-AIMS program^{61,62} using the light basis set and a 18 × 18 × 18 k-point grid. Scalar relativistic effects were included, where needed, through the zeroth-order relativistic approximation (ZORA).⁶³

3. RESULTS

In this section, we report the performance of PBE-like functionals using different values of the μ and κ parameters. For each test, the results are reported as a two-dimensional plot showing the mean absolute error (MAE) as a function of μ and κ . In the figures also the combinations of (μ, κ) corresponding to PBE, APBE, revPBE, and mPBEsol are indicated for reference. Here, mPBEsol indicates a functional having the same (μ, κ) values as the original PBEsol^{37,38} ($\mu = 10/81$, $\kappa = 0.804$), but a different value of β (0.037) imposed by the constraint of the LSDA response satisfaction. Actually, this functional was already considered in ref 41, where it was indicated as PBE(J_x, G_x), yielding a very similar performance with the original PBEsol.

In the following discussion, we will also compare the results of the PBE-like functional with other common ones, i.e., BLYP,^{64,65} OLYP,^{65–67} PBEint,⁴⁴ TPSS meta-GGA,⁶⁸ and the global hybrid PBE0.⁶⁹ These results are reported in Table S1, in the Supporting Information.

To discuss the performances of different functionals, we introduce an exchange (X) nonlocality measure Λ for PBE-like functionals. The true nonlocality of a GGA functional is given by the XC enhancement factor $F_{XC}(r_s, \zeta_s)$.⁷⁰ However, this function

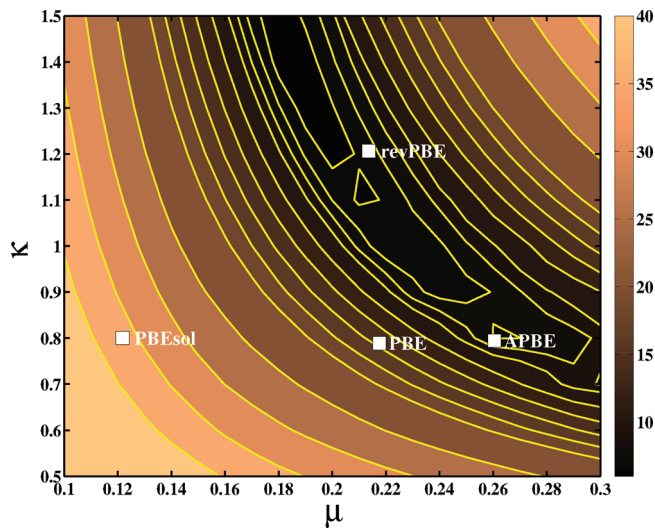


Figure 1. Mean absolute error (kcal/mol) for the atomization energy of molecules of the AE6 set as a function of μ and κ . The positions corresponding to PBE, APBE, revPBE, and mPBESol are denoted by white boxes.

of three variables is too complicated to yield a simple measure, as the one required in this work. For this reason, we consider simply $F_{XC}(r_s = 0, \zeta = 0, s) = F_X(s)$, i.e., the leading exchange part. For a given functional, the X-nonlocality is thus defined as

$$I_{\text{func}} \equiv \int_0^{s_{\max}} (F_{\text{func}}(s) - 1) ds \quad (7)$$

where F is the enhancement factor of the functional and s_{\max} is the maximum value of the reduced gradient s that contributes to the integration of the exchange energy (eq 4). Here, we used $s_{\max} = 6$; however, our final result will turn out to be independent of the value of s_{\max} provided that it is large enough. Using the PBE-like exchange enhancement factor form (eq 3), performing the integration, and after some algebra, we find

$$I_{\text{func}} = \frac{\kappa_{\text{func}}^2}{\sqrt{\mu_{\text{func}} \kappa_{\text{func}}}} G\left(\frac{\mu_{\text{func}} s_{\max}}{\sqrt{\mu_{\text{func}} \kappa_{\text{func}}}}\right) \quad (8)$$

with $G(x) = x - \arctan(x)$. In the range of μ and κ values considered in this work, we can approximate the function G as

$$G(x) \approx \frac{x^2}{c s_{\max}} \quad (9)$$

where $c = 1.05$ is a fitting parameter. The X-nonlocality of the functional can thus be written as

$$I_{\text{func}} = \frac{\sqrt{\mu_{\text{func}} \kappa_{\text{func}}} s_{\max}}{c} \quad (10)$$

The X-nonlocality measure can be finally defined as the X-nonlocality of the given functional relative to PBE, i.e.

$$\Lambda_{\text{func}} = \frac{I_{\text{func}}}{I_{\text{PBE}}} = \frac{\sqrt{\mu_{\text{func}} \kappa_{\text{func}}}}{\sqrt{\mu_{\text{PBE}} \kappa_{\text{PBE}}}} \quad (11)$$

The values of the X-nonlocality measure for the different PBE-like functionals considered in this paper are reported in Figure S1, in the Supporting Information. For standard PBE-like

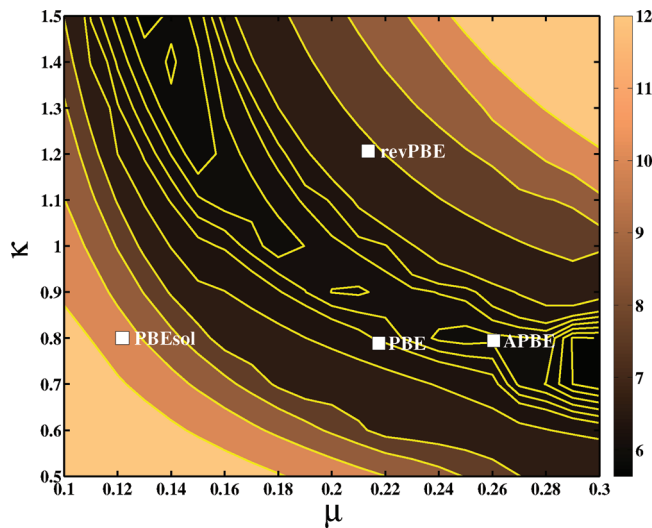


Figure 2. Mean absolute error (kcal/mol) for the atomization energy of the TMAE4 set, as a function of μ and κ . The positions corresponding to PBE, APBE, revPBE, and mPBESol are denoted by white boxes.

functionals, we have 0.75, 1.00, 1.09, and 1.24 for mPBESol, PBE, APBE, and revPBE, respectively.

3.1. Molecules. *3.1.1. Atomization Energies.* In Figure 1, we report the MAE for the AE6 test as a function of μ and κ . The best results, with MAEs below 10 kcal/mol, are found for combinations of the two parameters including either high values of κ and intermediate values of μ or intermediate values of κ and high values of μ . Both the APBE (MAE 7.9 kcal/mol) and the revAPBE (MAE 8.84 kcal/mol) functionals belong to this region and indeed yield for this test a performance close to the best GGAs (e.g., OLYP^{65–67} has a MAE of 4.3 kcal/mol) and to the TPSS⁶⁸ meta-GGA (MAE 5.4 kcal/mol) and hybrid PBE0⁶⁹ functional (MAE 5.4 kcal/mol).

The PBE functional lays just outside the region of minimum MAEs and gives a mean absolute error of 14.5 kcal/mol. A very poor performance for the AE6 test is found, as expected, for the mPBESol functional, which strongly overestimates atomization energies, because of its reduced X-nonlocality ($\Lambda_{\text{mPBESol}} = 0.75$).

Interestingly, the PBE performance can be improved, increasing the X-nonlocality by either increasing the value of the μ parameter, yielding APBE ($\Lambda_{\text{APBE}} = 1.09$), or increasing the value of the κ parameter, yielding revPBE ($\Lambda_{\text{revPBE}} = 1.24$). However, a too pronounced X-nonlocality (functionals in the top-right region of Figure 1) makes the result worse (significant underestimation). This appears also from the comparison of APE and revPBE results. Indeed, the values of μ and κ defining the APBE functional correspond approximately to a minimum for the MAE of the AE6 test.¹²

In Figure 2, we show the MAE for the TMAE4 test as a function of μ and κ . A similar trend is observed as in the case of the AE6 test, but the region with lower MAE is shifted toward lower μ and κ . Thus, a slightly lower X-nonlocality of the functionals is required: in fact, the smaller errors (about 6–7 kcal/mol) are obtained for functionals with $\Lambda \sim 1.04–1.1$. This finding is not surprising, as the TMAE4 test considers large atoms. In fact, even a slightly lower nonlocality might be expected to be needed if larger systems are considered.⁷¹

Both the PBE (MAE 6.3 kcal/mol) and APBE (MAE 6.1 kcal/mol) functionals perform very well and better than the

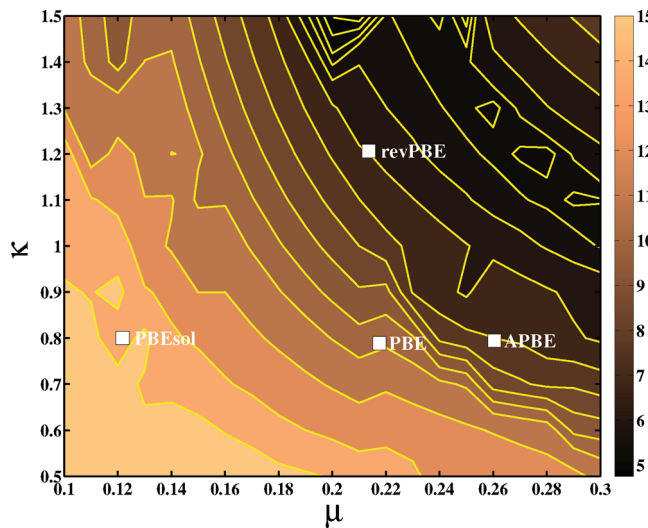


Figure 3. Mean absolute error (kcal/mol) for the atomization energy of the MCAE6 test set, as a function of μ and κ . The positions corresponding to PBE, APBE, revPBE, and mPBEsol are denoted by white boxes.

TPSS meta-GGA functional (MAE 6.6 kcal/mol). The revPBE functional yields a MAE that is about 1.5 kcal/mol higher than PBE, mainly because of its excessive X-nonlocality, given by a too high value of the κ parameter in combination with $\mu = 0.2195$. On the other hand, the mPBEsol functional yields again a rather poor result (overestimated atomization energies), because of its too low degree of X-nonlocality.

In Figure 3, the MAE for the MCAE6 test is shown. Unlike the previous two tests, in this case, a higher level of X-nonlocality is necessary to appropriately describe the metal complexes' atomization energies. The region of the minima is in fact significantly moved toward the top-right corner of the plot, corresponding to PBE-like functionals with $\Lambda \sim 1.35$. None of the commonly used PBE-like functionals possesses such a high level of X-nonlocality, and therefore none of them yields results close to the best possible performance. The smallest MAE is found with the revPBE functional (MAE 6.3 kcal/mol), which improves with respect to PBE because of the higher value of κ , and it is close to the best GGA, i.e., OLYP with a MAE of 5.4 kcal/mol. Rather good results are also found for the APBE functional (MAE 7.4 kcal/mol), which performs better than TPSS (MAE 7.7 kcal/mol) and PBE0 (MAE 10.3 kcal/mol). The PBE functional gives instead a MAE of 10.5 kcal/mol and turns out to be unable to provide a completely reliable description of these systems. Finally, mPBEsol displays very poor performance (overestimating atomization energies).

To have a global assessment of all atomization energies, in Figure 4, we report the global mean absolute error for the atomization energies of the AE6, TMAE4, and MCAE6 test sets, normalized to the PBE value (taken as a reference value), i.e.

$$\text{GMAE}(\mu, \kappa) = \frac{1}{3} \sum_i \frac{\text{MAE}_i(\mu, \kappa)}{\text{MAE}_i(\text{PBE})} \quad (12)$$

where i runs over AE6, TMAE4, and MCAE6. An inspection of the figure shows that for the GMAE there exists an almost continuous distribution of minima, all with very similar GMAEs (about 0.7). The locus of these minima can be

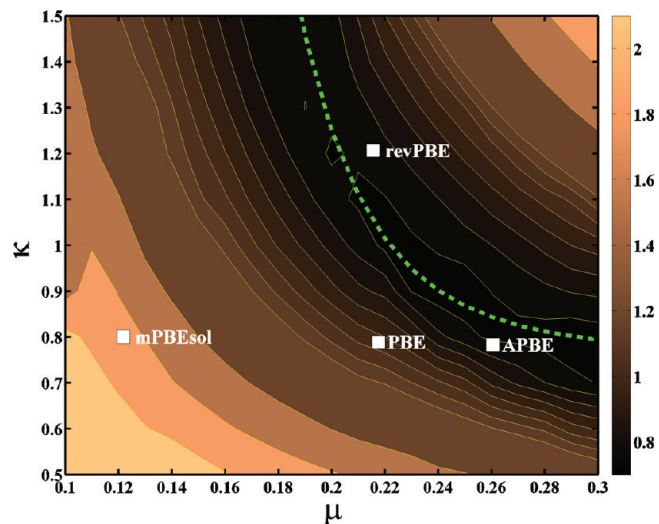


Figure 4. Global mean absolute error for the atomization energies of AE6, TMAE4, and MCAE6, normalized to the PBE value. The positions corresponding to PBE, APBE, revPBE, and mPBEsol are denoted by white boxes. The family of functionals defined by eq 13 is shown with a green line.

described well by the relation

$$\kappa = a + \frac{b}{\mu^\gamma} \quad (13)$$

with $a = 0.7457$, $b = 6.532 \times 10^{-6}$, and $\gamma = 6.968$. Equation 13 defines a family of PBE-like functionals optimized for the atomization energies of molecular systems and is shown in Figure 4 as a green dashed-line. We note that eq 13 was obtained considering test sets including only small molecules; therefore, it may be expected to reflect a slight preference for moderately high levels of nonlocality. Indeed, the need for a slightly reduced nonlocality in PBE-like functionals was already evidenced in the case of gold nanostructures of increasing size.⁷¹ Moreover, eq 13 is only a simple empirical fit to the data of Figure 4; therefore, it cannot be employed to obtain accurate numerical results (note also that eq 13, because of its form, is prone to numerical noise). Nevertheless, we can use eq 13 to discuss some important results:

- (i) For accurate atomization energies, κ displays a lower bound ($\kappa \geq a = 0.7457$) close to the nonempirical κ^{PBE} . Thus, we can extrapolate that a PBE-like functional with $\mu \rightarrow \infty$ and $\kappa = a = 0.7457$ will give extremely high total energies of atoms and molecules but still will be accurate for atomization energies. This shows that the atomization energies are dominated by the valence regions where the reduced gradient is relatively big ($s \geq 2$).
- (ii) For $\mu = \mu^{\text{GE2}} = 10/81$, we can extrapolate $\kappa \approx 14.7$ (eq 13 might not be very accurate in this region; thus, the following discussion is only qualitative). This very large value of κ violates largely the Lieb–Oxford bound⁴⁸ and has little physical meaning, showing that accurate atomization energies cannot be recovered by any reasonable PBE-like functional when $\mu = \mu^{\text{GE2}}$ (they can be however obtained by relaxing slightly the PBE form, as in the PBEint functional⁴⁴). Additionally, we note that a functional with $\mu = \mu^{\text{GE2}}$ and $\kappa \approx 14.7$ would yield very overestimated total energies and also extremely poor

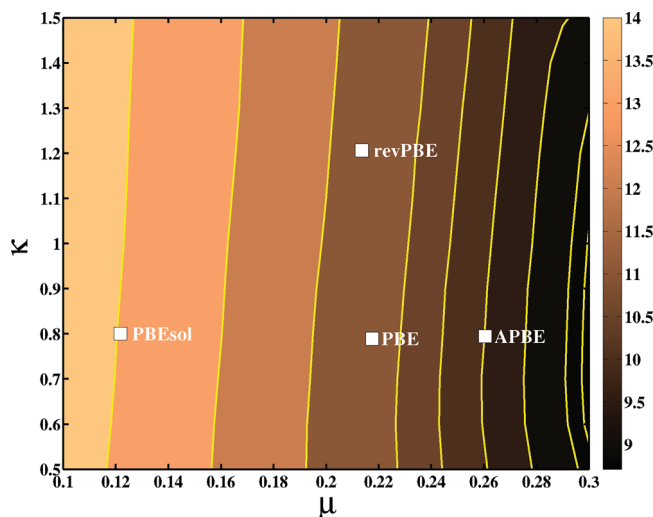


Figure 5. Mean absolute error ($\text{m}\text{\AA}$) for the equilibrium bond lengths of the HBL9 test set, as a function of μ and κ . The positions corresponding to PBE, APBE, revPBE, and mPBEsol are denoted by white boxes.

results for solid-state systems, worsening much over mPBEsol because of its very high X-nonlocality measure ($\Lambda = 3.2$).

- (iii) Both APBE and revPBE are practically members of the PBE-like family defined by eq 13. APBE is however closer to the curve than revPBE. In fact, the GMAE for atomization energies (see eq 12) is 0.74 and 0.82 for APBE and revPBE, respectively.
- (iv) The functionals defined by eq 13, although yielding very similar global MAEs for the atomization energies, possess a very different X-nonlocality measure. Using eqs 11 and 13, we find in fact $\Lambda_{(\mu, \kappa)} = (a\mu + b/\mu^{\gamma-1})^{1/2}/(\mu_{\text{PBE}}\kappa_{\text{PBE}})^{1/2}$, which is very high for small values of μ and close to 1.1 for $0.22 \leq \mu \leq 0.3$ (it has a minimum of 1.094 at $\mu = 0.243$). This implies that only the functionals with a relatively high value of the μ parameter, and correspondingly $\kappa \sim 0.8$, e.g., APBE, can be expected to work well for atomization energies as well as for problems that require a rather reduced level of X-nonlocality such as bond lengths and solid-state properties (see later).

3.1.2. Bond Lengths. To perform an assessment for the bond lengths of organic molecules, we divided the systems of the MGBL19⁵⁴ into two groups: The HBL9 test set contains bonds that involve at least one hydrogen atom; the NHBL10 test set instead contains only bonds which do not involve hydrogen. The two sets in fact turn out to have completely different behaviors and need to be analyzed separately (see Figure S2 in the Supporting Information).

In Figure 5, we report the results of the HBL9 test for the bond lengths of several organic molecules containing hydrogen. In this case, unlike for the atomization energies, the results of the test do not appear to be directly related to the X-nonlocality measure of the functionals, and the figure does not show the characteristic hyperbolic pattern of the previous cases. The results are almost independent from the value of the κ parameter and only vary with μ . In more detail (see Figure S2 in Supporting Information), using higher values of μ leads to a reduction of the bond lengths, especially for the H–H bond. Thus, because all of the bond

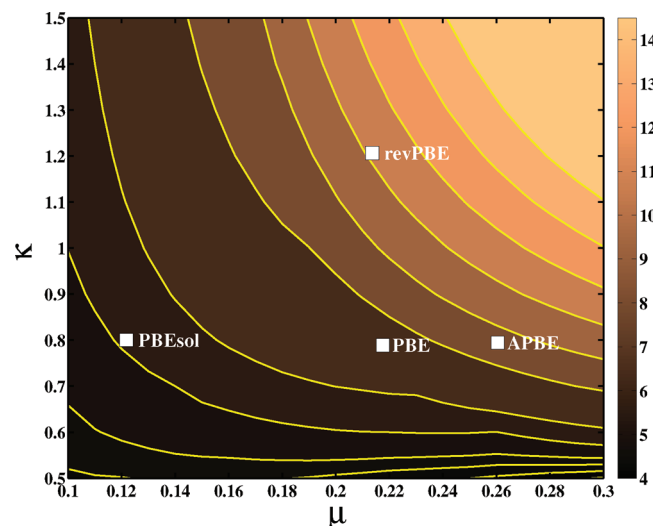


Figure 6. Mean absolute error ($\text{m}\text{\AA}$) for the equilibrium bond lengths of the NHBL10 test set, as a function of μ and κ . The positions corresponding to PBE, APBE, revPBE, and mPBEsol are denoted by white boxes.

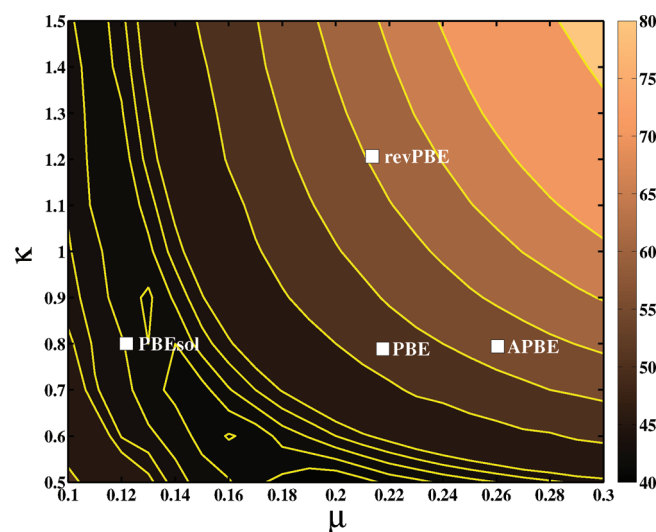


Figure 7. Mean absolute error ($\text{m}\text{\AA}$) for the equilibrium bond lengths of the TMBL4 test set, as a function of μ and κ . The positions corresponding to PBE, APBE, revPBE, and mPBEsol are denoted by white boxes.

lengths in this test are generally overestimated, a better agreement with the reference values is found at high μ . As a result, the smallest MAE is found, for standard PBE-like functionals, at the APBE level, with 9.6 $\text{m}\text{\AA}$.

In Figure 6, we report the results of the NHBL10 test for the bond lengths of several organic molecules, excluding bonds with hydrogen atoms. The plot, in contrast to Figure 5, shows the characteristic hyperbolic pattern already observed for the atomization energies and indicates that the best performance is achieved by functionals having a rather small X-nonlocality measure. Among the standard PBE-like functionals, in fact, mPBEsol yields the smallest MAE (5.6 $\text{m}\text{\AA}$), while the worst results are obtained by revPBE (MAE 11.1 $\text{m}\text{\AA}$). The bond distances in the NHBL10 test set are all increased when the

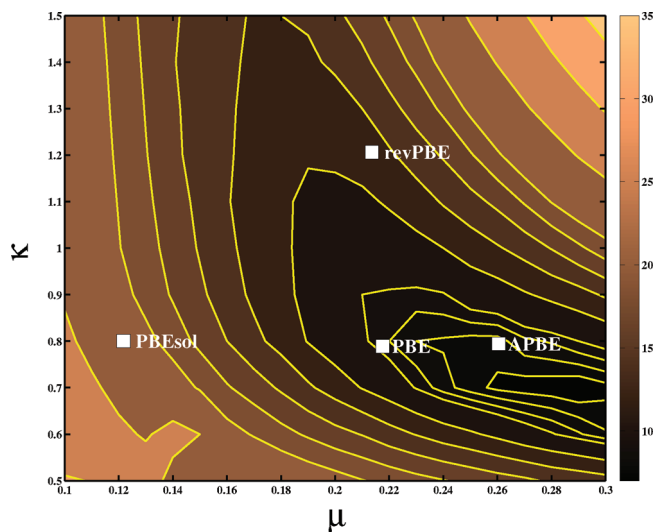


Figure 8. Mean absolute error ($\text{m}\text{\AA}$) for the equilibrium bond lengths of the MCBL6 test set, as a function of μ and κ . The positions corresponding to PBE, APBE, revPBE, and mPBEsol are denoted by white boxes.

X-nonlocality of the functional is increased (see Figure S2 in the Supporting Information). Since for small values of the X-nonlocality measure most bonds are very well described, this causes a worsening of the accuracy for high values of the X-nonlocality.

Because of the different behavior of the two tests with respect to the variations of μ and κ , good results cannot be achieved at the same time for both sets. The best performance for all organic molecules (i.e., the whole MGBL19 test) is obtained overall for high values of μ and very low values of κ (see Figure S3 in the Supporting Information), because this combination best balances the two opposing trends. In this case, MAEs of about 6.5 $\text{m}\text{\AA}$ are obtained, which compare well with the results of TPSS (MAE 6.9 $\text{m}\text{\AA}$) and PBE0 (MAE 6.3 $\text{m}\text{\AA}$) calculations. PBE, mPBEsol, and APBE give all the same accuracy, while revPBE works quite badly (MAE 11.4 $\text{m}\text{\AA}$).

Considering together atomization energy and bond length for organic molecular systems, Figure S4 in the Supporting Information shows that APBE is the best choice ($\text{MAE}_{\text{APBE}}/\text{MAE}_{\text{PBE}} = 0.78$). APBE not only outperforms both PBE and revPBE but it has the maximum accuracy among all of the PBE-like functionals considered.

The MAEs of the bond lengths of the TMBL4 test set as functions of μ and κ are shown in Figure 7. The best results are found when small values of the μ parameter are considered and, despite the fact that when this condition is satisfied, the MAE is rather independent of the value of the κ parameter, in general a low X-nonlocality is needed ($\Delta < 1$). Thus, the use of a small κ (~ 0.6) and medium-small μ (~ 0.16) yields the smallest error for bond lengths with a MAE of 40.9 $\text{m}\text{\AA}$. This error compares favorably with that obtained using the TPSS meta-GGA functional (MAE 42.6 $\text{m}\text{\AA}$). Very large errors are found on the other hand for functionals exploiting a high level of X-nonlocality.

According to this analysis, among the standard PBE-like functionals, the mPBEsol functional yields the best performance for the description of bond lengths of transition metal dimers (MAE 43.1 $\text{m}\text{\AA}$). Note that mPBEsol was instead very bad for the atomization energies of these systems (TMAE4; Figure 2). Larger errors are found in the order PBE (MAE 52.8 $\text{m}\text{\AA}$) and APBE (MAE 57.3 $\text{m}\text{\AA}$), because of the increasing X-nonlocality of the functionals. The revPBE functional yields finally the

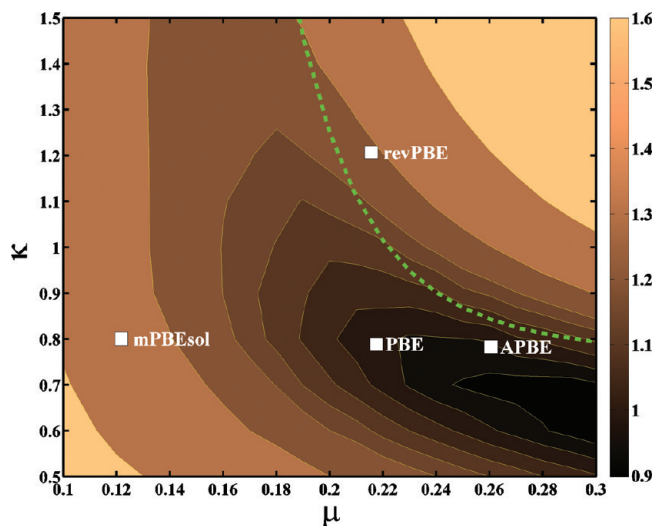


Figure 9. Global mean absolute error for the bond lengths of MGBL19, TMBL4, and MCBL6, normalized to the PBE value. The positions corresponding to PBE, APBE, revPBE, and mPBEsol are denoted by white boxes. The family of functionals defined by eq 13 is shown with a green line.

poorest performance with a MAE of 62.2 $\text{m}\text{\AA}$. While mPBEsol is the best for TMBL4, it was the worst for TMAE4. Considering together atomization and bond length for transition metal systems, Figure S5 in the Supporting Information shows that PBE and APBE yield high and comparable accuracy, outperforming both mPBEsol and revPBE. In this case, however, Figure S5 shows that the best functional should have μ as in mPBEsol but a very high κ .

In Figure 8, we report the results of the MCBL6 test on the bond lengths of six metal complexes. The smallest mean average errors are found for combinations of μ and κ , giving a medium value of the X-nonlocality measure $\Delta \sim 1$, i.e., for relatively high values of the μ parameter and $\kappa \sim 0.7/0.8$. The APBE and PBE functionals thus perform well with a MAE of 8.3 and 9.2 $\text{m}\text{\AA}$, respectively. For comparison, MAEs of 8.1 and 14.2 $\text{m}\text{\AA}$ are found at the TPSS and PBE0 levels, respectively. The revPBE (MAE 14.5 $\text{m}\text{\AA}$) and mPBEsol (MAE 22.4 $\text{m}\text{\AA}$) functionals yield instead significantly worse results because of the too large/small X-nonlocality of revPBE/mPBEsol. Considering together atomization energies and bond lengths for metal complexes, Figure S6 in the Supporting Information shows that APBE has the maximum accuracy ($\text{MAE}_{\text{APBE}}/\text{MAE}_{\text{PBE}} = 0.80$) among all of the PBE-like functionals considered.

Figures 5–8 show overall that for bond lengths, a more important role is played by the value of the μ parameter, which must be high for HBL10 and MCBL6 and small for TMBL4, while the value of the κ parameter is less important. Moreover, a moderate/small level of X-nonlocality is requested to obtain accurate results. The importance of μ traces back to the fact that for bond lengths a fundamental role is played by the first derivative of the XC potential with respect to the nuclear positions, which is related in the present context to the derivative of the exchange enhancement factor with respect to s^2 . This latter term, once the X-nonlocality measure of the functional is fixed ($\mu/\kappa \approx \text{const.}$), depends in first approximation only on μ , which is then mainly determining the performance of the functionals for the problem.

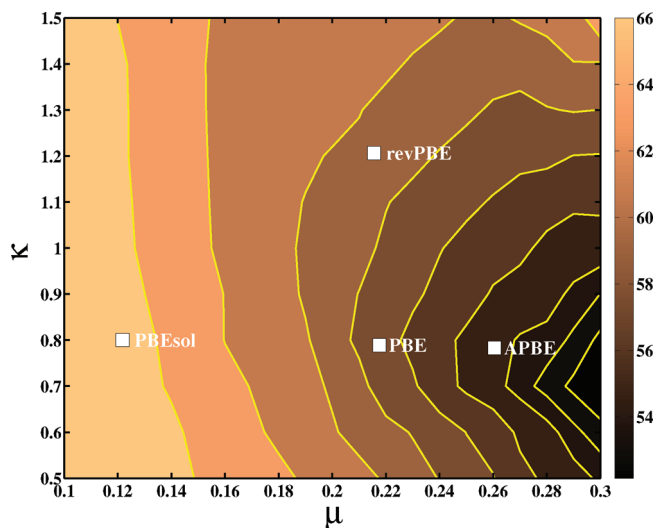


Figure 10. Mean absolute error (cm^{-1}) for the vibrational frequencies of molecules of the F38 test set, as a function of μ and κ . The positions corresponding to PBE, APBE, revPBE, and mPBEsol are denoted by white boxes. The family of functionals defined by eq 13 is shown with a green line.

The overall performance of different PBE-like functionals for the computation of equilibrium bond lengths is summarized in Figure 9, where we report the global MAE for the bond lengths tests (see eq 12). Because different values of μ are required by different tests, in this case, we do not find a full family of PBE-like functionals with the same and high accuracy. Instead, the best performance corresponds to a well-defined region at site $0.25 < \mu < 0.3$ and $0.6 < \kappa < 0.7$. Therefore, among the commonly used PBE-like functionals, the best results are given by APBE with a GMAE (with respect to PBE) of 0.99. Note, however, that the global performance for bond lengths results mainly from an error balancing between the values obtained for the organic molecules and the transition-metal dimers.

As previously discussed, the APBE functional provides also the best compromise for the simultaneous accurate calculations of bond lengths and atomization energies (see Figures S4–S6 in the Supporting Information). Finally, APBE is also the best functional considering together atomization energies and bond lengths of all molecular systems, with a GMAE (with respect to PBE) of 0.82 (see Figure S7 in the Supporting Information).

3.1.3. Vibrational Frequencies. For molecular systems, we also consider harmonic vibrational frequencies (the F38 test). First of all, we note that Figure 10 does not show a hyperbolic pattern, but a strong dependence of the functionals' performance from the value of the μ parameter and a minor role of the κ value. This finding can be explained, in analogy with the case of bond lengths where the first derivative of the exchange enhancement factor was important, by the importance of the second derivative of the enhancement factor for harmonic vibrations. This term in fact is, in first approximation, linearly dependent on the μ parameter and independent from the κ parameter (once the X-nonlocality of the functional is fixed, in this case, to a moderate value $\Lambda \sim 1.1$).

Moreover, we observe that all of the functionals belonging to the PBE family yield similar results, with maximum differences on the order of 10 cm^{-1} , irrespective of the values used for μ and κ . None of the combinations of μ and κ considered in this work proved to be able to yield very accurate results.

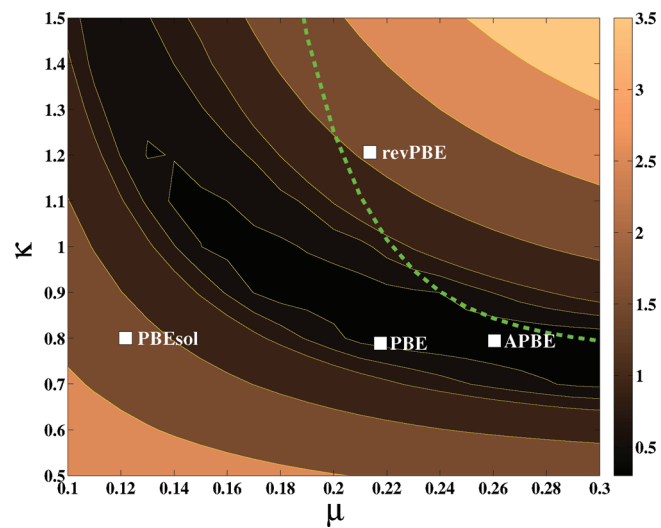


Figure 11. Mean absolute error (kcal/mol) for the binding energies of the HB6/04 benchmark test of hydrogen-bond interacting systems, as a function of μ and κ . The positions corresponding to PBE, APBE, revPBE, and mPBEsol are denoted by white boxes.

In fact, the minimum MAE in Figure 10 is 52 cm^{-1} , while the best GGA and hybrid methods give much smaller errors (e.g., OLYP MAE is 40.1 cm^{-1} , B3LYP MAE is 33 cm^{-1}).⁵⁵ However, ref 55 shows that F38 is well described only by the nonlocal rungs of Jacob's ladder (e.g., double-hybrids with a MAE of 18 cm^{-1}), whereas the semilocal rungs (including meta-GGAs) give in general modest accuracy, so they cannot be used in spectroscopic studies.

PBE-like functionals with high values of the μ parameter and $\kappa \sim 0.7$ display the best performance, while poor results are found for small values of μ , for any κ value. As a consequence, among the standard PBE-like functionals, the smallest MAE is obtained with the APBE functional (55.0 cm^{-1}), and the worst result is achieved by the mPBEsol functional (67.4 cm^{-1}).

3.1.4. Nonbonded Interaction. Despite the fact that GGA functionals cannot correctly describe nonbonded interactions due to the missing/incorrect dispersion forces,⁷² very good performances were obtained by the PBE functional for hydrogen-bond and dipole–dipole interaction systems.⁵⁶

In Figure 11, we report the plot of the MAE of HB6/04 binding energies (kcal/mol) as a function of μ and κ . In this case, the plot resembles the one for atomization energies. In fact, both of them are total energy differences between interacting and noninteracting subsystems.

The best results are obtained from functionals displaying a medium X-nonlocality measure ($\Lambda \sim 1/1.1$), while a too high/too low X-nonlocality leads to poor results, corresponding to a general underestimation/overestimation of the interaction energy. The absolute minimum in our plot is found for the APBE functional ($\mu = 0.26$, $\kappa = 0.8$) with a MAE of 0.32 kcal/mol . Note that this is, to our knowledge, the best performance in the literature for the hydrogen-bond problem,⁵⁶ twice as good as the best meta-GGA (TPSS MAE is 0.60 kcal/mol) and slightly better than the best hybrid functionals (PBE0 MAE 0.42 kcal/mol). Good results are obtained also from the PBE functional (MAE 0.38 kcal/mol), while poor results are found from revPBE (MAE 1.90 kcal/mol) and mPBEsol (MAE 1.86 kcal/mol) calculations.

In Figure 12, we report the MAE of DI6/04 binding energies (kcal/mol) as a function of μ and κ . A similar behavior as for the

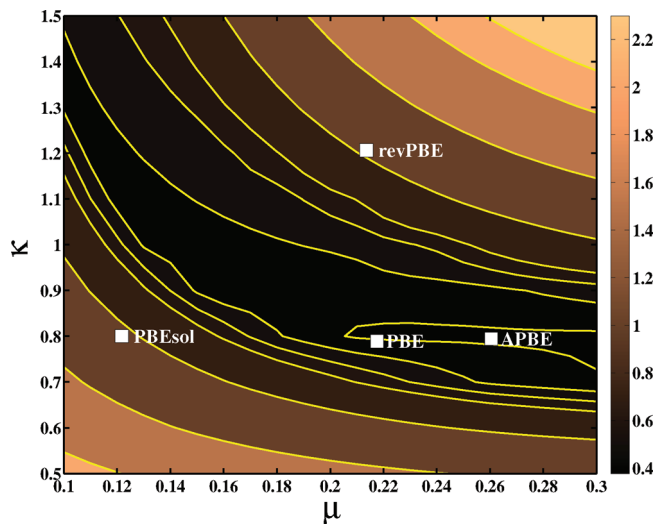


Figure 12. Mean absolute error (kcal/mol) for the binding energies of the DI6/04 benchmark test of dipole interacting systems, as a function of μ and κ . The positions corresponding to PBE, APBE, revPBE, and mPBEsol are denoted by white boxes.

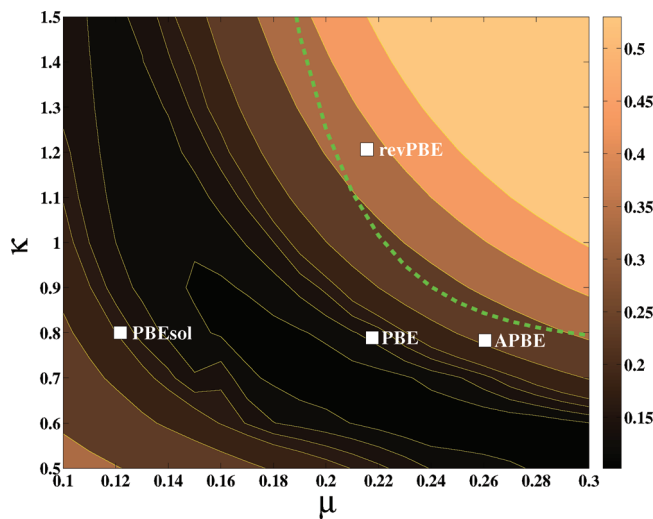


Figure 13. Mean absolute error (eV/atom) for the cohesive energies of six solids, as a function of μ and κ . The positions corresponding to PBE, APBE, revPBE, and mPBEsol are denoted by white boxes. The family of functionals defined by eq 13 is shown with a green line.

HB6/04 test is obtained, with functionals characterized by a medium X-nonlocality measure ($\lambda \sim 1$) performing best, while functionals with a high/low degree of X-nonlocality tend to underestimate/overestimate the interaction energy.

The PBE and APBE functionals yield the same MAE (0.38 kcal/mol), while larger errors are found for revPBE (1.22 kcal/mol) and mPBEsol (1.09 kcal/mol). The results obtained from the PBE and APBE functionals are among the best achievable at the GGA level,⁵⁶ comparable with the best meta-GGA functionals and slightly worse than the best hybrid approaches.⁵⁶

3.2. Solid State. In this section, we report briefly on the performance of PBE-like functionals for the description of equilibrium properties of solid-state systems. In particular, we focus on lattice constants and cohesive energies.

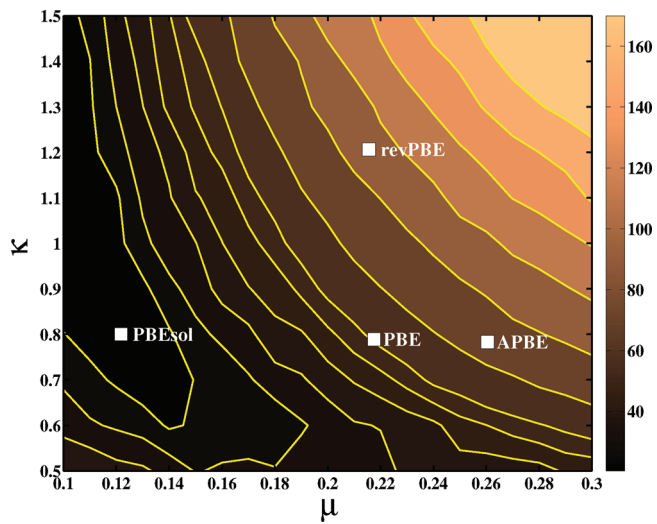


Figure 14. Mean absolute error (mÅ) for the lattice constants of six solids, as a function of μ and κ . The positions corresponding to PBE, APBE, revPBE, and mPBEsol are denoted by white boxes.

3.2.1. Cohesive Energies. In Figure 13, we report the MAE of the cohesive energies of six solids as a function of μ and κ . The plot resembles roughly that of Figure 2, where the performances for the atomization energies of transition metal dimers are reported. The cohesive energy of a bulk solid (of the chemical element Y) seems in fact to be the upper bound of the atomization energy of any neutral cluster of the same chemical element.^{71,73} However, in the bulk, the density is more slowly varying than in molecular systems, and thus the set of functionals given by eq 13 becomes too nonlocal (see Figure 13). The smaller errors are obtained for functionals with a relatively small X-nonlocality measure ($\Lambda \sim 0.9$). This value of the X-nonlocality is in fact needed to provide balance between the description of the bulk solid, which is well described by rather local functionals, and the description of isolated atoms, which require a larger X-nonlocality in the functional.

Good results are obtained from the PBE functional with a MAE of 0.15 eV/atom. The mPBEsol functional instead yields a MAE of 0.21 eV/atom, because of its poor performance for the atomic energies. On the other hand, high errors are also obtained from APBE (MAE 0.26 eV/atom) and revPBE (MAE 0.41 eV/atom), because of the too high X-nonlocality included in these functionals. We note finally that both PBE and APBE performance can be improved reducing κ , as found in ref 40.

3.2.2. Lattice constants. In Figure 14, we consider the ability of PBE-like functionals with different μ and κ values to describe the lattice constant of different solids. The best performance is obtained for the functionals characterized by small values of μ and in general by a low X-nonlocality. In fact, for higher values of μ , reasonably small MAEs are found in conjunction with very small values of κ , while large errors are obtained when both μ and κ are large. These findings resemble the results of the bond lengths of transition metal dimers (Figure 7).

The mPBEsol functional is the best standard PBE-like functional for this problem with a MAE of 19 mÅ, while the revPBE functional yields very poor results (MAE 105 mÅ). Large errors (overestimated bond-lengths) are also found at the PBE (MAE 60 mÅ) and APBE (MAE 79 mÅ) levels because of the too high value of μ and X-nonlocality in these two functionals. We note

that mPBEsol represents almost a global minimum on the plot of Figure 14 and can thus be hardly improved for this property within the PBE GGA form.

Many studies have been carried out for the construction of accurate GGAs for solids. The AM05 GGA⁷⁴ was constructed using the Airy gas, the uniform electron gas, and the jellium surfaces as reference systems. The PBEsol GGA, instead, recovers the second-order gradient expansion of the exchange energy, which is the right, exact constraint for solids, as also shown in Figure 14. Several other GGAs for solids have been proposed in refs 36, 40, 41, 46, and 75, and all of them have a reduced X-nonlocality, showing small gradient corrections to LSDA for small values of s . We recall that LSDA is remarkably accurate for solid-state physics. In particular, when μ is fixed to $\mu = \mu_{\text{PBE}} = 0.2195$, the following values of κ are needed for accurate lattice constants: $\kappa \approx 0.5$ for 4d transition metals, $\kappa \approx 0.3$ for 5d transition metals, $\kappa \sim \kappa^{\text{PBE}} = 0.804$ for 3d metals.⁷⁵

4. SUMMARY AND GLOBAL RESULTS

In the previous section, we conducted a survey of the PBE-like functionals with different (μ, κ) parameters (fixing $\beta = 3\mu/\pi^2$), for a broad set of tests and properties of molecular and solid-state systems. We have shown that different requirements are necessary in order to have PBE-like functionals accurate for different energetic or structural properties of molecules or solids. In this section, we summarize global results for molecular and solid-state systems. In order to be able to compare the performance of different functionals for different problems, we will normalize all MAEs to the PBE value; i.e., we will consider $\text{MAE}/\text{MAE}(\text{PBE})$ for each property and functional and use these to compute a global MAE, denoted MAE_{PBE} .

For molecular properties, including atomization energies, bond lengths, harmonic vibrational frequencies, and noncovalent interaction energies, we found that PBE-like functionals displaying a medium X-nonlocality ($\Lambda \sim 1/1.1$) yield the best overall performance thanks to the right balance between situations where a relatively small X-nonlocality is favored (TMAE4, bond lengths) and problems where a higher X-nonlocality is needed (AE6, MCAE6). The APBE functional is thus the best one when a global average is considered, with a $\text{MAE}_{\text{PBE}} = 0.90$ (see Table S1 in the Supporting Information), showing performance superior to that of PBE ($\text{MAE}_{\text{PBE}} = 1.00$), TPSS ($\text{MAE}_{\text{PBE}} = 0.91$), and the hybrid functionals (e.g., MAE_{PBE} of PBE0 = 1.32). The performance of the latter is very poor because it largely fails for transition metal dimers. This finding confirms the importance of the semiclassical neutral atom as the reference system used in the construction of APBE, for molecules.¹² The revPBE functional can give accurate atomization energies, although it only outperforms APBE for MCAE6 but is not accurate for bond lengths and noncovalent interactions. Thus, it gives a total MAE_{PBE} of 1.7, showing severe limitations for broad applicability in molecular calculations. Finally, the mPBEsol functional yields a MAE_{PBE} of 1.97, demonstrating its limits for the description of molecular properties.

For solid-state properties, a lower level of X-nonlocality is required, and the best overall performance is obtained with functionals having $\Lambda \sim 0.85$. This value constitutes a balance between the requirements of the cohesive-energy problem (medium X-nonlocality) and the lattice-constant determination (low X-nonlocality). Among the standard PBE-like functionals, the best overall performance is obtained with the mPBEsol

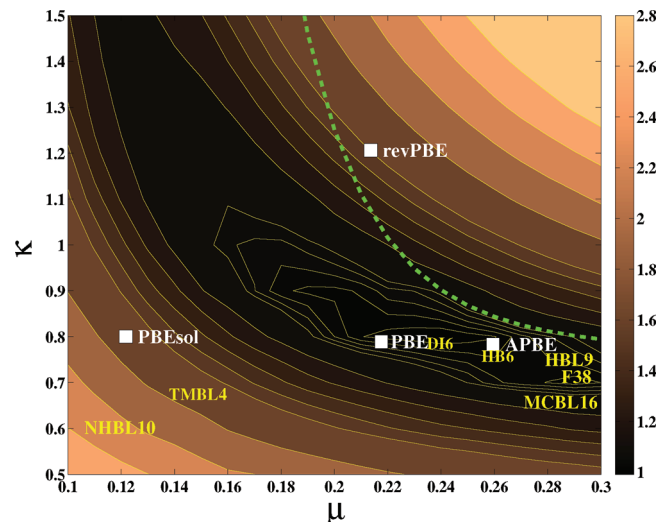


Figure 15. Global mean absolute error for all properties, normalized to the PBE value. The positions corresponding to PBE, APBE, revPBE, and mPBEsol are denoted by white boxes. The family of functionals defined by eq 13 is shown with a green line.

functional, having a MAE_{PBE} of 0.85 (see Table S2 in the Supporting Information). This originates mainly from its excellent performance for lattice constants, while not so accurate results are obtained for cohesive energies at the mPBEsol level. The opposite occurs for PBE, which shows the smallest MAE for the cohesive energies but an error 3 times larger than that of mPBEsol for lattice constants. In fact, a very good overall performance is obtained using the PBEint functional ($\text{MAE}_{\text{PBE}} = 0.76$), which can correctly describe the slowly varying density regime, relevant for lattice constants and partly for cohesive energies, and the rapidly varying density limit, which is essential for the description of atomic energies used to evaluate the cohesive energies. Similar results for the PBEint functional were already found concerning the energy and structural properties of metal clusters.⁷¹

To conclude, we report in Figure 15, the global mean absolute error of all properties and test sets, normalized to the PBE value. This plot shows why PBE has been the workhorse of electronic calculations for more than a decade: this nonempirical functional shows in fact almost the best average accuracy for a large number of properties of different systems, resulting in a good choice in almost any electronic-structure problem. This finding supports the idea behind the construction of the PBE functional, which is based on a wise selection of the most important exact constraints of the exchange-correlation energy for both molecules and solids. The same global average performance is also found for the APBE functional, which has the same global MAE as PBE. Larger values of MAE_{PBE} are instead found for revPBE (1.74) and mPBEsol (1.85), which do not show a broad applicability but must be instead considered specialized functionals.

We note also that, among the standard PBE-like functionals, APBE is the one which is closer, in the (μ, κ) space, to the largest number of minima for different problems considered in this work (the name of each test in Figure 15 indicates approximately the position of the corresponding minimum MAE). This means that, within these functionals, it is the one that yields the best MAE for the largest number of the properties. On the other hand, APBE

has a lower accuracy for NHBL10 and TMBL4, which require a low level of X-nonlocality.

In conclusion, the APBE functional proved to be very accurate for molecular properties, competing with meta-GGA and hybrid approaches. This result confirms the importance of the recent work on semiclassical theory,^{7–11} which brought new frontiers in density functional theory. It supports especially the role of the modified second-order gradient expansion (MGE2),^{9,11} built from the semiclassical neutral atom theory, which can be used at the GGA level as a powerful tool for the development of XC and kinetic energy functionals.¹²

The results presented in this work are of great importance for the assessment of PBE-like GGA XC functionals and to understand the merits and limitations of the presently available PBE-like approximations. We showed in fact the existence of an interrelation between the values of the μ and κ parameters, which must balance each other for the best performance, and the importance of considering properly the X-nonlocality measure of the functionals. The former property was recently also evidenced for kinetic energy functionals with the PBE-like form.⁷⁶ Thus, the present results can serve as a guide for the development and optimization of density functionals, in search of approximations having higher accuracy and broader applicability. However, it appears from the present study that there is little room for improvement within the PBE functional form, and new developments must be based on more flexible GGA expressions or based on higher rungs of the DFT Jacob's ladder. We recall that the nonempirical meta-GGAs (TPSS,⁶⁸ revTPSS,^{49,77} and JS⁷⁸) as well the hyper-GGA¹³ have all been constructed using the PBE functional form. Moreover, optimization of the μ parameter in the TPSS functional form⁷⁹ (that is responsible for the behavior of the meta-GGA at large s) revealed that the use of $\mu^{\text{APBE}} = 0.26$ improves over the original TPSS for the atomization energies of molecules, the molecular enthalpies of formation, and the barrier heights without worsening the XC jellium surface energies.⁷⁹ Thus, further work needs to be done for implementing the APBE ideas in meta- and hyper-GGAs.

■ ASSOCIATED CONTENT

Supporting Information. Two-dimensional plot of the X-nonlocality measure as a function of μ and κ , tests of atomization and interaction energies with β parameter fixed to 0.06672, performance for individual bond lengths of organic molecules, global performance for bond lengths of organic molecules, global performance for molecular systems, global performance for organic molecules, global performance for transition-metal dimers, global performance for organic-metal complexes, global performance for solid-state systems, and results for selected functionals. This information is available free of charge via the Internet at <http://pubs.acs.org/>.

■ AUTHOR INFORMATION

Corresponding Author

*E-mail: eduardo.fabiano@nano.cnr.it

■ ACKNOWLEDGMENT

We thank TURBOMOLE GmbH for providing us with the TURBOMOLE program package and M. Margarito for technical support. This work was funded by the ERC Starting Grant FP7 Project DEDOM, Grant Agreement No. 207441.

■ REFERENCES

- (1) Hohenberg, P.; Kohn, W. *Phys. Rev.* **1964**, *136*, B864.
- (2) Parr, R. G.; Yang, W. *Density-Functional Theory of Atoms and Molecules*; Oxford University Press: Oxford, 1989; pp 1–331.
- (3) Kohn, W.; Sham, L. *Phys. Rev.* **1965**, *140*, A1133.
- (4) Perdew, J. P.; Schmidt, K. In *Density Functional Theory and Its Application to Materials*; Van Doren, V. E., Van Alsenoy, K., Geerlings, P., Eds.; American Institute of Physics: Melville, 2001; pp 1–207.
- (5) Langreth, J. P., D. C.; Perdew *Phys. Rev. B* **1980**, *21*, 5469.
- (6) Antoniewicz, P. R.; Kleinman, L. *Phys. Rev. B* **1985**, *31*, 6779–6781.
- (7) Elliot, P.; Lee, D.; Cangi, A.; Burke, K. *Phys. Rev. Lett.* **2008**, *100*, 256406.
- (8) Cangi, A.; Lee, D.; Elliot, P.; Burke, K. *Phys. Rev. Lett.* **2010**, *81*, 235128.
- (9) Elliot, P.; Burke, K. *Can. J. Chem.* **2009**, *87*, 1485.
- (10) Perdew, J. P.; Constantin, L. A.; Sagvolden, E.; Burke, K. *Phys. Rev. Lett.* **2006**, *97*, 223002.
- (11) Lee, D.; Constantin, L. A.; Perdew, J. P.; Burke, K. *J. Chem. Phys.* **2009**, *130*, 034107.
- (12) Constantin, L. A.; Fabiano, E.; Laricchia, S.; Della Sala, F. *Phys. Rev. Lett.* **2011**, *106*, 186406.
- (13) Perdew, J. P.; Staroverov, V. N.; Tao, J.; Scuseria, G. E. *Phys. Rev. A* **2008**, *78*, 052513.
- (14) Becke, A. D. *J. Chem. Phys.* **1993**, *98*, 5648.
- (15) Kümmel, S.; Kronik, L. *Rev. Mod. Phys.* **2008**, *80*, 3.
- (16) Gritsenko, O. V.; Baerends, E. J. *Phys. Rev. A* **2001**, *64*, 042506.
- (17) Della Sala, F.; Görling, A. *J. Chem. Phys.* **2001**, *115*, 5718.
- (18) Grabowski, I.; Hirata, S.; Ivanov, S.; Bartlett, R. J. *J. Chem. Phys.* **2002**, *116*, 4415–4425.
- (19) Furche, F.; Voorhis, T. V. *J. Chem. Phys.* **2005**, *122*, 164106.
- (20) Fabiano, E.; Della Sala, F. *J. Chem. Phys.* **2007**, *126*, 214102.
- (21) Schimka, L.; Harl, J.; Stroppa, A.; Grüneis, A.; Marsman, M.; Mittendorfer, F.; Kresse, G. *Nat. Mater.* **2010**, *9*, 741.
- (22) Ruzsinszky, A.; Perdew, J. P.; Csonka, G. I. *J. Chem. Theory Comput.* **2010**, *6*, 127–134.
- (23) Ren, X.; Tkatchenko, A.; Rinke, P.; Scheffler, M. *Phys. Rev. Lett.* **2011**, *106*, 153003.
- (24) Koch, W.; Holthausen, M. C. *A Chemist's Guide to Density Functional Theory*; Wiley-VCH: New York, 2001; pp 1–293.
- (25) Schultz, N. E.; Zhao, Y.; Truhlar, D. G. *J. Phys. Chem. A* **2005**, *109*, 4388–4403 PMID: 16833770..
- (26) Schultz, N. E.; Zhao, Y.; Truhlar, D. G. *J. Phys. Chem. A* **2005**, *109*, 11127–11143.
- (27) Furche, F.; Perdew, J. P. *J. Chem. Phys.* **2006**, *124*, 044103.
- (28) Perdew, J. P.; Burke, K.; Ernzerhof, M. *Phys. Rev. Lett.* **1996**, *77*, 3865.
- (29) Perdew, J. P.; Burke, K.; Wang, Y. *Phys. Rev. B* **1996**, *54*, 16533–16539.
- (30) Becke, A. D. *J. Chem. Phys.* **1986**, *84*, 4524–4529.
- (31) Oliver, G. L.; Perdew, J. P. *Phys. Rev. A* **1979**, *20*, 397–403.
- (32) Zhang, Y.; Yang, W. *Phys. Rev. Lett.* **1998**, *80*, 890.
- (33) Hammer, B.; Hansen, L. B.; Nørskov, J. K. *Phys. Rev. B* **1999**, *59*, 7413–7421.
- (34) Adamo, C.; Barone, V. *J. Chem. Phys.* **2002**, *116*, 5933–5940.
- (35) Xu, X.; W. A., G., III *J. Chem. Phys.* **2004**, *121*, 4068–4082.
- (36) Wu, Z.; Cohen, R. E. *Phys. Rev. B* **2006**, *73*, 235116.
- (37) Perdew, J. P.; Ruzsinszky, A.; Csonka, G. I.; Vydrov, O. A.; Scuseria, G. E.; Constantin, L. A.; Zhou, X.; Burke, K. *Phys. Rev. Lett.* **2008**, *100*, 136406.
- (38) Perdew, J. P.; Ruzsinszky, A.; Csonka, G. I.; Vydrov, O. A.; Scuseria, G. E.; Constantin, L. A.; Zhou, X.; Burke, K. *Phys. Rev. Lett.* **2009**, *102*, 039902.
- (39) Madsen, G. K. H. *Phys. Rev. B* **2007**, *75*, 195108.
- (40) Zhao, Y.; Truhlar, D. G. *J. Chem. Phys.* **2008**, *128*, 184109.
- (41) Pedroza, L. S.; da Silva, A. J. R.; Capelle, K. *Phys. Rev. B* **2009**, *79*, 201106.

- (42) Ruzsinszky, A.; Csonka, G. I.; Scuseria, G. E. *J. Chem. Theory Comput.* **2009**, *5*, 763–769.
- (43) Goerigk, L.; Grimme, S. *J. Chem. Theory Comput.* **2010**, *6*, 107–126.
- (44) Fabiano, E.; Constantin, L. A.; Della Sala, F. *Phys. Rev. B* **2010**, *82*, 113104.
- (45) Haas, P.; Tran, F.; Blaha, P.; Schwarz, K. *Phys. Rev. B* **2011**, *83*, 205117.
- (46) Haas, P.; Tran, F.; Blaha, P.; Pedroza, L. S.; da Silva, A. J. R.; Odashima, M. M.; Capelle, K. *Phys. Rev. B* **2010**, *81*, 125136.
- (47) Csonka, G. I.; Perdew, J. P.; Ruzsinszky, A.; Philipsen, P. H. T.; Lebègue, S.; Paier, J.; Vydrov, O. A.; Ángyán, J. G. *Phys. Rev. B* **2009**, *79*, 155107.
- (48) Odashima, M. M.; Capelle, K. *J. Chem. Phys.* **2007**, *127*, 054106.
- (49) Perdew, J. P.; Ruzsinszky, A.; Csonka, G. I.; Constantin, L. A.; Sun, J. *Phys. Rev. Lett.* **2009**, *103*, 026403.
- (50) Goerigk, L.; Grimme, S. *J. Chem. Theory Comput.* **2011**, *7*, 291–309.
- (51) Grimme, S. *Wiley Interdisciplinary Reviews: Computational Molecular Science* **2011**, *1*, 211–228.
- (52) Korth, M.; Grimme, S. *J. Chem. Theory Comput.* **2009**, *5*, 993–1003.
- (53) Lynch, B. J.; Truhlar, D. G. *J. Phys. Chem. A* **2003**, *107*, 8996–8999.
- (54) Zhao, Y.; Truhlar, D. G. *J. Chem. Phys.* **2006**, *125*, 194101.
- (55) Biczysko, M.; Panek, P.; Scalmani, G.; Bloino, J.; Barone, V. *J. Chem. Theory Comput.* **2010**, *6*, 2115–2125.
- (56) Zhao, Y.; Truhlar, D. G. *J. Chem. Theory Comput.* **2005**, *1*, 415–432.
- (57) Haas, P.; Tran, F.; Blaha, P. *Phys. Rev. B* **2009**, *79*, 085104.
- (58) TURBOMOLE V6.2, 2009, a development of University of Karlsruhe and Forschungszentrum Karlsruhe GmbH, 1989–2007, TURBOMOLE GmbH, since 2007; available from <http://www.turbomole.com> (accessed September 2011).
- (59) Weigend, F.; Furche, F.; Ahlrichs, R. *J. Chem. Phys.* **2003**, *119*, 12753.
- (60) Weigend, F.; Ahlrichs, R. *Phys. Chem. Chem. Phys.* **2005**, *7*, 3297.
- (61) Blum, V.; Gehrke, R.; Hanke, F.; Havu, P.; avu, V. H.; Ren, X.; Reuter, K.; Scheffler, M. *Comput. Phys. Commun.* **2009**, *180*, 2175–2196.
- (62) Havu, V.; Blum, V.; Havu, P.; Scheffler, M. *J. Comput. Phys.* **2009**, *228*, 8367–8379.
- (63) Faas, S.; Snijders, J. G.; van Lenthe, J. H.; van Lenthe, E.; Baerends, E. *J. Chem. Phys. Lett.* **1995**, *246*, 632–640.
- (64) Becke, A. D. *Phys. Rev. A* **1988**, *38*, 3098.
- (65) Lee, C.; Yang, W.; Parr, R. G. *Phys. Rev. B* **1988**, *37*, 785.
- (66) Handy, A. J.; Cohen, N. C. *Mol. Phys.* **2001**, *99*, 403.
- (67) Hoe, W.-M.; Cohen, A. J.; Handy, N. C. *Chem. Phys. Lett.* **2001**, *341*, 319–328.
- (68) Tao, J.; Perdew, J. P.; Staroverov, V. N.; Scuseria, G. E. *Phys. Rev. Lett.* **2003**, *91*, 146401.
- (69) Adamo, C.; Barone, V. *J. Chem. Phys.* **1999**, *110*, 6158.
- (70) Perdew, J. P.; Ernzerhof, M.; Zupan, A.; Burke, K. *J. Chem. Phys.* **1998**, *108*, 1522–1531.
- (71) Fabiano, E.; Constantin, L. A.; Della Sala, F. *J. Chem. Phys.* **2011**, *134*, 194112.
- (72) Tao, J.; Perdew, J. P.; Ruzsinszky, A. *Phys. Rev. B* **2010**, *81*, 233102.
- (73) Baletto, F.; Ferrando, R. *Rev. Mod. Phys.* **2005**, *77*, 371–423.
- (74) Armiento, R.; Mattsson, A. E. *Phys. Rev. B* **2005**, *72*, 085108.
- (75) Peltzer y Blancá, E. L.; Rodríguez, C. O.; Shitu, J.; Novikov, D. L. *Journal of Physics: Condensed Matter* **2001**, *13*, 9463.
- (76) Laricchia, S.; Fabiano, E.; Constantin, L. A.; Della Sala, F. *J. Chem. Theory Comput.* **2011**, *7*, 2439.
- (77) Perdew, J. P.; Ruzsinszky, A.; Csonka, G. I.; Constantin, L. A.; Sun, J. *Phys. Rev. Lett.* **2011**, *106*, 179902.
- (78) Constantin, L. A.; Chiodo, L.; Fabiano, E.; Bodrenko, I.; Della Sala, F. *Phys. Rev. B* **2011**, *84*, 045126.
- (79) Perdew, J. P.; Ruzsinszky, A.; Tao, J.; Csonka, G. I.; Scuseria, G. E. *Phys. Rev. A* **2007**, *76*, 042406.